



# Event-Triggered Adaptive Fixed-Time Trajectory Tracking Control for Stratospheric Airship

Peihao Sun<sup>1</sup> · Ming Zhu<sup>2</sup> · Yifei Zhang<sup>2</sup> · Tian Chen<sup>2</sup> · Zeiwei Zheng<sup>3</sup>

Received: 19 April 2024 / Revised: 12 August 2024 / Accepted: 20 August 2024  
© The Author(s), under exclusive licence to The Korean Society for Aeronautical & Space Sciences 2024

## Abstract

This paper proposes a trajectory tracking controller to address the issue of the unmeasurable airspeed of a stratospheric airship. First, we propose a fixed-time extended state observer in solving the issues of unknown disturbances and unmeasurable airspeed. Utilizing the sliding mode control and backstepping framework, a fixed-time convergent controller is designed in this paper. Then, the fixed-time controller is integrated with the event-triggered mechanism to decrease the actuation frequency of the actuator during the tracking of the predetermined trajectory. After that, we provide a proof that the observer error converges to zero within a fixed time and the semi-global fixed-time uniform ultimate boundedness of the closed-loop output feedback control system is proved by Lyapunov stability analysis. The simulation results validate the efficacy of the algorithm.

**Keywords** Stratospheric airship · Fixed-time control · Event-triggered control · Trajectory tracking · Adaptive control · Backstepping method

## 1 Introduction

Due to the stable meteorological conditions and electromagnetic properties of stratospheric space, the stratospheric flight platform has attracted the attention of many researchers in recent years. The stratospheric airship has set off a worldwide development boom because of its advantages of long residence time and low cost [13, 17], etc. However,

from the perspective of control engineering, the control of stratospheric airships faces many challenges and difficulties compared with fixed-wing or rotorcraft. First, compared to fixed-wing aircraft or rotary-wing drones, the control challenges of stratospheric airships lie in their immense volume and considerable inertia, which significantly increase the difficulty of their control. Furthermore, due to their complex structure and operating environment, the dynamic characteristics of airships often exhibit multivariate, nonlinear, and uncertain traits. This makes it difficult to establish an accurate mathematical model for stratospheric airships, and traditional control methods are often not directly applicable to their control systems. Therefore, this research aims to explore the control strategies and methods of stratospheric airships from the perspective of control engineering, to provide new ideas and solutions for addressing their control challenges.

There has been significant progress in the research of trajectory tracking for stratospheric airships in recent years, and now there exist relatively mature research achievements. In [21], by redefining velocity and configuration errors and utilizing the dynamic characteristics of the error system, a state feedback control law is designed to enhance the stability of airship trajectory tracking. In [23], a control framework that includes predictive control and sliding mode control is proposed to solve the trajectory tracking problem of stratospheric airships under state constraints. In [4], the adaptive

Communicated by Tae-Hun Kim.

✉ Yifei Zhang  
zyifei@buaa.edu.cn  
Peihao Sun  
sunpeihao@buaa.edu.cn  
Ming Zhu  
zhuming@buaa.edu.cn  
Tian Chen  
chentian@buaa.edu.cn  
Zeiwei Zheng  
zeweizheng@buaa.edu.cn

- <sup>1</sup> School of Aeronautic Science and Engineering, Beihang University, Beijing, China
- <sup>2</sup> Institute of Unmanned System, Beihang University, Beijing, China
- <sup>3</sup> School of Automation Science and Electrical Engineering, Beihang University, Beijing, China

sliding mode attitude controller was used to track the attitude, and the problem of asymmetric error-constrained vector field path tracking was solved. In [5], a robust controller with an inner-outer loop structure is designed to solve the underactuated problem of stratospheric airships by proposing a new control tracking strategy. In [28], a multi-loop control system is designed to address the problem of planar trajectory tracking for underactuated stratospheric airships, and the simulation verification of classic path flight is achieved. Many other control strategies for airships have been extensively researched in addition to trajectory tracking control, such as path following control [29–31] and control of airships with special structures [3, 11].

The aforementioned control methods are only capable of ensuring asymptotic convergence, meaning that there is no constraint on the convergence time of errors. However, in practical airship operations, the convergence time is a crucial performance metric. To address this concern, fixed-time control schemes [16] can offer a faster convergence rate, ensuring that the system error converges within each fixed time interval. In [27], for incomplete systems, a fixed-time control strategy is proposed based on the concept of power integration. In [22], by designing an integral sliding surface, an adaptive fixed-time control system is derived, but it is not extended to higher-order systems. In [14], by transformation extension, the error system is transformed from a time-delay system to a non-delay system, and a non-singular sliding mode is designed to achieve fixed-time uniform convergence. In [34], a cascade control structure is constructed to achieve fixed-time tracking control under external disturbances.

However, emphasizing solely on enhancing the controller's performance is insufficient from a broader perspective. In current technology level, stratospheric airships must adopt time-space energy storage strategies to achieve day-night cycling. Moreover, traditional onboard wind speed measurement equipment uses a Pitot tube [7]. For flights in the stratosphere with low air density and low power, the pressure changes caused by dynamic pressure cannot be accurately measured. Therefore, to meet the mission requirements, developing a control algorithm for stratospheric airships that can minimize energy consumption while effectively tracking trajectory in the absence of airspeed measurement has become an urgent problem to be solved.

During the long-term operation of the stratospheric airship, the duration of staying in the air is mainly affected by the battery power and the avionics equipment life, so the equipment loss should be reduced as much as possible. Therefore, event-triggered control can be utilized to decouple control tasks from time periodicity, thereby reducing the working frequency of the controller, achieving the goal of reducing energy consumption and improving the working lifespan. In [12], an event-triggered control based on fixed and variable thresholds is implemented for a suspension system using a

radial basis function neural network. In [24], they proposed an event-triggered mechanism to address the issue of communication load between the controller and the actuator in dynamic positioning of marine surface ships with actuator faults. In [6], a robust fuzzy control scheme based on event-triggered was proposed to ensure the high fidelity of the path tracking control of underactuated ships. In [8], by employing guided control event-triggered, the number of controller executions for a ship is reduced. In [33], the communication and computation burden of the path tracking controller of a watercraft has been reduced by using an event-triggered mechanism.

To address the issue of unmeasurable airspeed, methods such as adaptive control [18, 32], fuzzy logic systems [15], and neural networks [9] can be utilized in the design of control algorithms. In [18], minimizing the performance index of unmanned aerial vehicles is achieved through the design of a strictly negative imaginary part adaptive controller. In [15], this study achieved the guidance and obstacle avoidance of robots in unknown disturbances by using singleton fuzzy control and fuzzy blending control. In [9], under non-extreme conditions, unknown variables can be estimated by analyzing ship wakes using convolutional neural networks.

This paper is inspired by the works of [1, 20], and we address the issue of trajectory tracking in stratospheric airships. The paper integrates a fixed-time convergence controller and a fixed-time extended state observer with event-triggered mechanism to achieve the airship control task.

The main contributions and characteristics of the proposed method in this paper can be summarized as follows:

1. Drawing on the actual characteristics of stratospheric airships and practical control challenges, including unknown individual differences of airships, external interference, and limited communication and computing resources, this study addresses the problem of trajectory tracking control for stratospheric airships when the airspeed is unmeasurable. Furthermore, this study investigates the implementation of an event-triggered mechanism to enhance the operational lifespan of stratospheric airships.
2. The backstepping method is utilized to design virtual control laws for achieving trajectory tracking tasks. A filter is also designed to estimate the derivative of virtual state variables to reduce complex computations. Additionally, a fixed-time extended state observer is firstly designed, and an adaptive law is introduced to eliminate unknown terms, ensuring that each term in the state space complies with engineering practice. These methods contribute to enhancing the control performance of the system while reducing computational complexity.
3. By designing an event-triggered mechanism, the controller calculations will only be performed when the set

threshold conditions are met, significantly reducing the frequency of controller calculations and achieving the goal of saving computing resources.

This paper is arranged as follows. The mathematical model of the airship and the prior knowledge needed in the rest sections are shown in Sect. 2. The design of the observer and its convergence proof are shown in Sect. 3. In Sect. 4, the control law was designed by the backstepping method, and it was proved that the controller is semi-globally uniformly ultimately bounded. In Sect. 5, the paper presents simulation results. The full text is summarized, and the paper concludes by highlighting future work in Sect. 6.

## 2 Problem Formulation and Preliminaries

### 2.1 Problem Formulation

The stratospheric airship model in this paper is shown in Fig. 1.

The nonlinear mathematical model of the stratospheric airship with six DOF(degrees of freedom) is expressed as

$$\begin{cases} \dot{X}_1 = T X_2 \\ \dot{X}_2 = -\chi^{-1}(\Upsilon X_2 + \Gamma(v_a)) + \chi^{-1}\tau \end{cases} \quad (1)$$

where  $X_1 = [x, y, z, \phi, \theta, \varphi]^T$  is the 6-DOF position attitude vector of the stratospheric airship,  $X_2 = [u, v, w, p, q, r]^T$  is the 6-DOF velocity and angular velocity information of the stratospheric airship.  $\chi$  is a constant value symmetric matrix,  $\Upsilon$  denotes the inertial matrix.  $v_a$  is the airspeed.  $\tau = [\tau_u, \tau_v, \tau_w, \tau_p, \tau_q, \tau_r]^T$  corresponds to the forward thrust, lateral thrust, longitudinal thrust, roll adjustment moment, pitch adjustment moment, and yaw adjustment moment of the airship, respectively.  $T$  is the rotation matrix given as

$$\begin{aligned} T &= \begin{bmatrix} R & 0_{3 \times 3} \\ 0_{3 \times 3} & K \end{bmatrix}, \\ R &= \begin{bmatrix} c\theta c\psi & s\theta c\psi s\phi - s\psi c\phi & s\theta c\psi c\phi + s\psi s\phi \\ c\theta s\psi & s\theta s\psi s\phi + c\psi c\phi & s\theta s\psi c\phi - c\psi s\phi \\ -s\theta & c\theta s\phi & c\theta c\phi \end{bmatrix}, \\ K &= \begin{bmatrix} 1 & s\phi t\theta & c\phi t\theta \\ 0 & c\phi & -s\phi \\ 0 & s\phi e\theta & c\phi e\theta \end{bmatrix}, \end{aligned} \quad (2)$$

where  $s \cdot = \sin \cdot, c \cdot = \cos \cdot, t \cdot = \tan \cdot, e \cdot = \sec \cdot$ . Obviously can obtain that  $\|T\| = \frac{1}{\cos\theta} \geq 1$  and  $\|\cdot\|$  means the determinant of a matrix.

**Remark 1** Since the airspeed is unmeasurable,  $\Gamma(v_a)$  in the Eq. (1) is an unknown quantity to be estimated, and the math-

ematical expression is

$$\begin{aligned} \Gamma(v_a) &= \begin{bmatrix} (G - B) \sin \theta - F_{ax} \\ (B - G) \cos \theta \sin \phi - F_{ay} \\ (B - G) \cos \theta \cos \phi - F_{az} \\ z_C G \cos \theta \sin \phi - y_C G \cos \theta \cos \phi - M_{ax} \\ z_C G \sin \theta + x_C G \cos \theta \cos \phi - M_{ay} \\ -x_C \cos \theta \sin \phi - y_C G \sin \theta - M_{az} \end{bmatrix}, \\ F_a &= \begin{bmatrix} -\frac{1}{2}\rho v_a^2 S_{ref} C_x(\alpha_{angle}, \beta_{sideslip}, q, r) \\ -\frac{1}{2}\rho v_a^2 S_{ref} C_y(\beta_{sideslip}, q, r) \\ -\frac{1}{2}\rho v_a^2 S_{ref} C_z(\alpha_{angle}, q, r) \end{bmatrix} \Rightarrow \begin{bmatrix} F_{ax} \\ F_{ay} \\ F_{az} \end{bmatrix}, \\ M_a &= \begin{bmatrix} -\frac{1}{2}\rho v_a^2 S_{ref} L_{ref} C_l(\alpha_{angle}, \beta_{sideslip}, p, \dot{p}) \\ -\frac{1}{2}\rho v_a^2 S_{ref} L_{ref} C_m(\alpha_{angle}, \beta_{sideslip}, p, \dot{p}, q, \dot{q}) \\ -\frac{1}{2}\rho v_a^2 S_{ref} L_{ref} C_n(\alpha_{angle}, \beta_{sideslip}, p, \dot{p}, r, \dot{r}) \end{bmatrix} \\ &\Rightarrow \begin{bmatrix} M_{ax} \\ M_{ay} \\ M_{az} \end{bmatrix}, \end{aligned}$$

where the gravity force on the airship is  $G = mg$ , the buoyancy force is  $B = \rho g \nabla$ ,  $\nabla$  is the total volume of the airship,  $\rho$  is the atmospheric density at the altitude of the airship,  $g$  is the acceleration of gravity at the altitude of the airship.  $F_{ax}, F_{ay}, F_{az}$  and  $C_x, C_y, C_z$  are the drag, drag coefficient, lateral force, lateral force coefficient, lift, and lift coefficient of the airship, respectively.  $M_{ax}, M_{ay}, M_{az}$  and  $C_l, C_m, C_n$  are the roll moment, pitch moment, yaw moment and the corresponding coefficient of the airship, respectively.  $S_{ref}$  is the reference area,  $L_{ref}$  is the reference length.

The more detailed model derivation is given in [4].

**Assumption 1** The control input  $F_T$  and  $M_T$  satisfies  $F_{T,\min} \leq F_T \leq F_{T,\max}, M_{T,\min} \leq M_T \leq M_{T,\max}$ . It can be obtained that the control input  $t$  satisfies the input constraint as

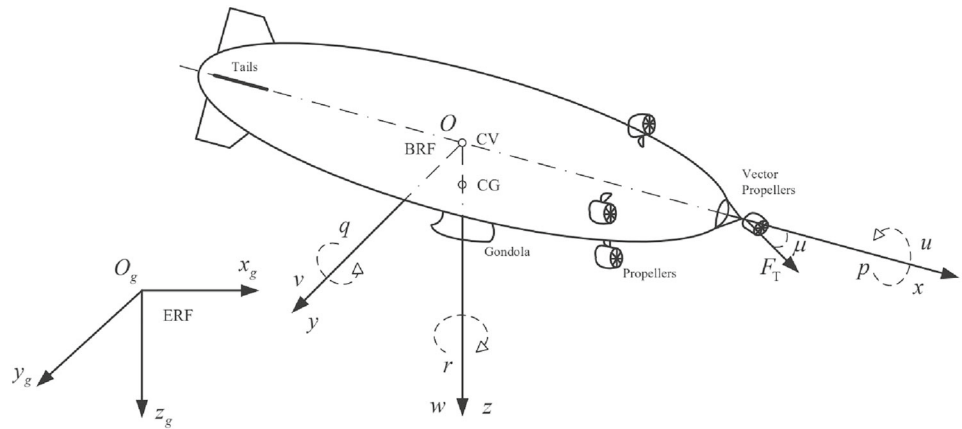
$$\begin{aligned} \tau &= \text{sat}(\tau_0) \\ &= \begin{cases} \tau_{0,\max}, & \tau_0 > \tau_{0,\max} \\ \tau_0, & \tau_{0,\min} \leq \tau_0 \leq \tau_{0,\max} \\ \tau_{0,\min}, & \tau_0 < \tau_{0,\min} \end{cases} \\ &= \tau_0 + \delta_\tau, \end{aligned} \quad (3)$$

where  $\cdot_{\max}$  and  $\cdot_{\min}$  denote the maximum and minimum value of the control input, respectively.

**Assumption 2** The desired position  $X_{1d}$  of an airship is bounded and differentiable second order.

**Assumption 3** The airspeed of the airship is unmeasurable. Due to the thin air in the stratosphere, the vast majority of

**Fig. 1** Structure of the stratospheric airship



stratospheric airships cannot effectively measure airspeed. The target pose is artificially set, so the assumption is valid.

## 2.2 Preliminaries

For an  $n$ -dimensional vector  $\mathbf{x}$  we have  $\text{sig}^a(\mathbf{x}) = [|x_1|^a \text{sign}(x_1), |x_2|^a \text{sign}(x_2), \dots, |x_n|^a \text{sign}(x_n)]$ ,  $\text{sign}(\mathbf{x}) = [\text{sign}(x_1), \text{sign}(x_2), \dots, \text{sign}(x_n)]$ , where  $a$  is an arbitrary real number,  $\text{sign}(\cdot)$  is the sign function as

$$\text{sign}(x) = \begin{cases} -1 & x < 0 \\ 0 & x = 0 \\ 1 & x > 0 \end{cases} \quad (4)$$

For a nonlinear system  $\mathbf{x}(t)$ ,  $\mathbf{x} = [x_1, x_2, \dots, x_n]$  satisfies

$$\begin{aligned} \dot{\mathbf{x}}(t) &= f(\mathbf{x}(t)), \\ \mathbf{x}(0) &= \mathbf{0} \\ f(0) &= \mathbf{0}, \mathbf{x} \in R^n, \end{aligned} \quad (5)$$

where  $R^n$  is an  $n$ -dimensional vector.

$\boldsymbol{\theta}$  and  $\boldsymbol{\theta}^k$  are expressed as  $\boldsymbol{\theta} = [\theta_1, \theta_2, \dots, \theta_n]^T$ ,  $\boldsymbol{\theta}^k = [\theta_1^k, \theta_2^k, \dots, \theta_n^k]^T$ .

**Lemma 1** [20] If Eq. (5) is satisfied as

$$\begin{aligned} \dot{\mathbf{x}} &= -c_1 \text{sig}^\alpha(\mathbf{x}) - c_2 \text{sig}^\beta(\mathbf{x}), \\ \mathbf{x}(0) &= \mathbf{0}, \end{aligned} \quad (6)$$

where  $\alpha, \beta, c_1, c_2$  are positive constants and satisfy  $0 < \alpha < 1, \beta > 1$ , then this nonlinear system is fixed-time convergent and the convergence time  $T$  is satisfied as

$$T \leq \frac{1}{c_1(1-\alpha)} + \frac{1}{c_2(\beta-1)}. \quad (7)$$

In addition, if there exist small perturbations such that the nonlinear system of equation (5) is satisfied as

$$\dot{\mathbf{x}} = -c_1 \text{sig}^\alpha(\mathbf{x}) - c_2 \text{sig}^\beta(\mathbf{x}) + \boldsymbol{\eta}, \mathbf{x}(0) = \mathbf{x}_0, \quad (8)$$

where  $\boldsymbol{\eta}$  is a vector of small positive real numbers, then this nonlinear system is semi-global fixed-time uniform ultimate boundedness (SGFTUUB), and it converges in the neighborhood of the origin, and the convergence time is satisfied as

$$T \leq \frac{1}{c_1(1-\alpha)(2^\alpha-1)} + \frac{1}{c_2(\beta-1)}. \quad (9)$$

## 3 Observer Design

### 3.1 Model Transformation

The paper's proposed event-triggered mechanism  $\bar{\boldsymbol{\tau}} = \text{sat}(\boldsymbol{\tau}_0)$ ,  $\boldsymbol{\tau}(t) = \bar{\boldsymbol{\tau}}(t_k), \forall t \in [t_k, t_{k+1})$  is defined as

$$\begin{aligned} t_{k+1} &= \inf \{ t > t_k \mid |e_1(t)| \geq \zeta_1 |\bar{\tau}_1(t_k)| + \varsigma_1 \text{ or} \\ &\quad |e_2(t)| \geq \zeta_2 |\bar{\tau}_2(t_k)| + \varsigma_2 \text{ or} \\ &\quad \vdots \\ &\quad |e_6(t)| \geq \zeta_6 |\bar{\tau}_6(t_k)| + \varsigma_6 \}, \end{aligned}$$

where  $e_i(t) = \tau_i(t) - \bar{\tau}_i(t_k)$  is the measurement error.  $0 < \zeta_i < 1$  and  $\varsigma_i > 0$  are controller parameters.

**Remark 2** Definition  $\varphi_i(t) = \frac{\bar{\tau}_i(t) - \tau_i(t)}{\zeta_i |\bar{\tau}_i(t)| + \varsigma_i}$ ,  $i = 1, 2, \dots, 6$ , according to the trigger condition, for any  $t \in [t_k, t_{k+1})$ , there are  $\bar{\tau}_i(t) - \tau_i(t) \leq \zeta_i |\bar{\tau}_i(t_k)| + \varsigma_i$ , and  $\tau_i(t) = \bar{\tau}_i(t_k)$ ,  $|\varphi_i(t)| \leq 1, k = 0, 1, 2, \dots$  are attainable by definition  $t_0 := 0$ . The controller error caused by event-triggered mechanism is defined as  $\varrho_i(t) := \bar{\tau}_i(t) - \tau_i(t)$ . From  $|\varphi_i(t)| \leq 1, \bar{\tau}_{i,\min} \leq \bar{\tau}_i(t) \leq \bar{\tau}_{i,\max}$ , the error  $\varrho_i(t)$  is bounded.

From the event-triggered mechanism we have

$$\bar{\tau}(t) = \varphi(t)(\zeta|\tau(t)| + \varsigma) + \tau(t), \tag{10}$$

where  $\varphi, \zeta, \varsigma$  are the parameters to be designed, and the bounded error  $\varrho(t)$  caused by event-triggered mechanism can be eliminated by the adaptive term.

For ease of calculation, let

$$\delta^* = \chi^{-1}\Gamma(v_a) + f + \chi^{-1}\varrho + \delta_\tau, \tag{11}$$

where  $f$  is the external disturbance.

Consider the (10) and (11), the observer model are expressed as

$$\begin{cases} \dot{X}_1 = TX_2 \\ \dot{X}_2 = -\chi^{-1}\Upsilon X_2 + \chi^{-1}\bar{\tau} + \delta^*. \end{cases} \tag{12}$$

**Assumption 4** From Remark 2, the error  $\varrho_i(t)$  is bounded. The external disturbance terms  $\Gamma$  and  $f$  are continuous and bounded.

**Assumption 5** Since the perturbation in the stratospheric environment is significantly smaller than that in the tropospheric environment, and the motor power is limited, the perturbation does not change much, there is a constant  $C$  such that  $\|\delta^*\| \leq C$  holds.

### 3.2 Fixed-Time Convergence Observer

The observer is designed as follows

$$\begin{cases} \dot{\hat{X}}_1 = T\hat{X}_2 + \mu_1\text{sig}^{\alpha_1}(X_1 - \hat{X}_1) + \varepsilon_1\text{sig}^{\beta_1}(X_1 - \hat{X}_1) \\ \dot{\hat{X}}_2 = -\chi^{-1}\Upsilon X_2 + \chi^{-1}\bar{\tau} + \delta^* + \mu_2\text{sig}^{\alpha_2}(X_1 - \hat{X}_1) \\ \quad + \varepsilon_2\text{sig}^{\beta_2}(X_1 - \hat{X}_1) \\ \dot{\hat{\delta}}^* = \mu_3\text{sig}^{\alpha_3}(X_1 - \hat{X}_1) + \varepsilon_3\text{sig}^{\beta_3}(X_1 - \hat{X}_1) \\ \quad + \gamma_1\text{sig}^{1/2}(X_1 - \hat{X}_1) + \ell_1 \\ \dot{\ell}_1 = k_1\text{sign}(X_1 - \hat{X}_1), \end{cases} \tag{13}$$

where  $\ell_1$  is the adaptive term;  $\alpha_i \in (0, 1), \beta_i > 1, i = 1, 2, 3, 4; \mu_i, \varepsilon_i, \gamma_1, k_1$  are positive constants;  $\hat{X}_1, \hat{X}_2, \hat{\delta}^*$  are the observed values of the pose, velocity and disturbance, respectively.

The error of the observer is defined as

$$\begin{cases} \tilde{e}_1 = X_1 - \hat{X}_1 \\ \tilde{e}_2 = X_2 - \hat{X}_2 \\ \tilde{e}_3 = \delta^* - \hat{\delta}^*, \end{cases} \tag{14}$$

the derivative of Eq. (14) is as follows

$$\begin{cases} \dot{\tilde{e}}_1 = T\tilde{e}_2 - \mu_1\text{sig}^{\alpha_1}(\tilde{e}_1) - \varepsilon_1\text{sig}^{\beta_1}(\tilde{e}_1) \\ \dot{\tilde{e}}_2 = \tilde{e}_3 - \mu_2\text{sig}^{\alpha_2}(\tilde{e}_1) - \varepsilon_2\text{sig}^{\beta_2}(\tilde{e}_1) \\ \dot{\tilde{e}}_3 = \dot{\delta}^* - \mu_3\text{sig}^{\alpha_3}(\tilde{e}_1) - \varepsilon_3\text{sig}^{\beta_3}(\tilde{e}_1) - \gamma_1\text{sig}^{1/2}(\tilde{e}_1) \\ \quad - \ell_1. \end{cases} \tag{15}$$

The parameters  $\alpha_i = i\bar{\alpha} - (i - 1), \beta_i = i\bar{\beta} - (i - 1), \bar{\alpha} \in (1 - l_1), \bar{\beta} \in (1 + l_2)$  with small constants  $l_1 > 0, l_2 > 0$ . The observer gain  $\mu_i, \varepsilon_i, i = 1, 2, 3, 4$  are assigned such that the matrix  $A_1, A_2$  is Hurwitzian

$$A_1 = \begin{bmatrix} -\varepsilon_1 & 1 & 0 \\ -\varepsilon_2 & 0 & 1 \\ -\varepsilon_3 & 0 & 0 \end{bmatrix},$$

$$A_2 = \begin{bmatrix} -\mu_1 & 1 & 0 \\ -\mu_2 & 0 & 1 \\ -\mu_3 & 0 & 0 \end{bmatrix}.$$

Firstly, consider the error system (15) separately with the new forms only

$$\begin{cases} \dot{\tilde{e}}_1 = T\tilde{e}_2 - \mu_1\text{sig}^{\alpha_1}(\tilde{e}_1) - \varepsilon_1\text{sig}^{\beta_1}(\tilde{e}_1) \\ \dot{\tilde{e}}_2 = \tilde{e}_3 - \mu_2\text{sig}^{\alpha_2}(\tilde{e}_1) - \varepsilon_2\text{sig}^{\beta_2}(\tilde{e}_1) \\ \dot{\tilde{e}}_3 = \dot{\delta}^* - \mu_3\text{sig}^{\alpha_3}(\tilde{e}_1) - \varepsilon_3\text{sig}^{\beta_3}(\tilde{e}_1). \end{cases} \tag{16}$$

**Theorem 1** Based on Assumptions 1–4, the system (16) can converge to zero in finite time, and the convergence time is denoted as

$$T_1 \leq \frac{\lambda_{\max}^{1-\bar{\alpha}}(P_1)}{\gamma_1(1-\bar{\alpha})} + \frac{1}{\gamma_2(\bar{\beta}-1)\Psi^{\bar{\beta}-1}}, \tag{17}$$

where  $\gamma_1 = \lambda_{\min}(Q_1)/\lambda_{\max}(P_1), \gamma_2 = \lambda_{\min}(Q_2)/\lambda_{\max}(P_2). \Psi$  is a positive number satisfied as  $\Psi \leq \lambda_{\min}(P_2). P_1, P_2, Q_1, Q_2$  are positive definite nonsingular symmetric matrices and satisfied as  $P_1A_1 + A_1^T P_1 = -Q_1, P_2A_2 + A_2^T P_2 = -Q_2.$

**Proof** The main proof process refers to Theorem 2 of [1] and Theorem 1 of [25]. Consider two Lyapunov functions as  $V_1(\beta_1, e) = \kappa^T P_1 \kappa$  and  $V_2(\alpha_1, e) = \varpi^T P_2 \varpi$ , where  $e = [\tilde{e}_1, \tilde{e}_2, \tilde{e}_3^*]^T, \kappa = [e_1^{1/r_1}, e_2^{1/r_2}, e_3^{1/r_3}], \varpi = [e_1^{1/s_1}, \dots, e_3^{1/s_3}], s_i = (i - 1)\bar{\alpha} - (i - 2), r_i = (i - 1)\bar{\beta} - (i - 2); i = 1, 2, 3.$

Derivation of  $V_1$  at gain of  $\beta_1 = 1$  as

$$\begin{aligned} \dot{V}_1(1, e) &= \dot{\kappa}^T P_1 \kappa + \kappa^T P_1 \dot{\kappa} \\ &= \dot{e}^T P_1 e + e^T P_1 \dot{e} \\ &= e^T (P_1 A_1 + A_1^T P_1) e \\ &= -e^T Q_1 e \\ &\leq 0. \end{aligned} \tag{18}$$

**Remark 3** In Eq. (18),  $\kappa$  is regarded as a three-dimensional vector, but each element of it is also a three-dimensional vector. For the sake of mathematical rigor, the  $P_1$  matrix can be extended to a block diagonal matrix  $P_1^*$  with the same dimension as  $K$ ,

$$P_1^* = \begin{bmatrix} P_1 & \mathbf{0}_{3 \times 3} & \mathbf{0}_{3 \times 3} \\ \mathbf{0}_{3 \times 3} & P_1 & \mathbf{0}_{3 \times 3} \\ \mathbf{0}_{3 \times 3} & \mathbf{0}_{3 \times 3} & P_1 \end{bmatrix},$$

which does not affect the subsequent operation. Besides that, the elements in the Hurwitz matrix  $A_1$  are the observer parameters to be set, and no other variables are involved, so Eq. (18) holds.

According to (18), if  $e_i = \mathbf{0}$ , there is  $\dot{e}_i = \mathbf{0}$  and  $\dot{V}_1(1, e) = 0$ , it is worth noting that if  $\beta_1 \in (1, 1 + \xi)$  where  $\xi$  is a small constant, there is  $\dot{V}_1(\beta_1, e) \leq 0$ , the error system for  $V_1$  is asymptotically stable.

Based on this thought, according to theorem 7.1 in [2] we have

$$\dot{V}_1(\beta_1, e) \leq -(\lambda_{\min} Q_1 / \lambda_{\max} P_1) V_1^{\bar{\beta}}(\beta_1, e). \quad (19)$$

Similarly, the derivative of  $V_2(\alpha_1, e)$  with respect to time will be obtained

$$\dot{V}_2(\alpha_1, e) \leq -(\lambda_{\min} Q_2 / \lambda_{\max} P_2) V_2^{\bar{\alpha}}(\alpha_1, e). \quad (20)$$

From Rayleigh's inequalities:

$$\|\varpi\| \leq \frac{V_2(\varpi)}{\lambda_{\min} P_2} \leq \frac{\Omega}{\lambda_{\min} P_2} \leq 1 \quad (21)$$

and  $V_1(\kappa) \leq \lambda_{\max} P_1 \|\kappa\|^2$

applied to  $\|\kappa\| = 1$ . Take a number  $\Omega$  such that  $V_2(\varpi(t_0)) > \Omega$ , the full-time derivatives along the trajectory of the whole system (16) are calculated as

$$\dot{V}_2 \leq \dot{V}_2(\varpi) + \sum_{i=1}^n \frac{\partial(V_2)}{\partial x_i}(v_i(t)) \leq \dot{V}_2(\varpi) \leq -\gamma_2 V_2^{\bar{\alpha}}(\varpi), \quad (22)$$

where  $\gamma_2 = \lambda_{\min} Q_2 / \lambda_{\max} P_2$ , it is easy to prove that  $V_2$  convergence reaches  $\Omega$  in time no longer than  $T_2 = 1 / (\gamma_2(\bar{\beta} - 1)\Omega^{\bar{\beta}-1})$  which independent of the initial conditions of the system (16).

The full-time derivative of  $V(\kappa)$  along system trajectory (16) is calculated as

$$\dot{V}_1 \leq \dot{V}_1(\kappa) + \sum_{i=1}^n \frac{\partial(V_1)}{\partial x_i}(w_i(t)) \leq \dot{V}_1(\kappa) \leq -\gamma_1 V_1^{\bar{\beta}}, \quad (23)$$

where  $\gamma_1 = \lambda_{\min} Q_1 / \lambda_{\max} P_1$ .

For the term  $\delta^*$ , which is regarded as a small quantity mentioned in Lemma 1, we can see that it does not affect the convergence of fixed time if  $\alpha$  is sufficiently close to 1.  $\square$

**Remark 4** This paper only discusses the bounded error of the observer at the initial time.

Therefore, it can be concluded that (16) converges in a fixed time  $T_1$ ; according to the fixed-time convergence property, when  $t > T_1$ , the system is always in a convergent state, that is,  $\dot{e}_1 = \dot{e}_2 = \dot{e}_3 = \mathbf{0}$ ; substitute this conclusion into Eq. (13) as follows

$$\begin{cases} \dot{e}_1 = \mathbf{0} \\ \dot{e}_2 = \mathbf{0} \\ \dot{e}_3 = -\gamma_1 \text{sig}^{1/2}(\tilde{e}_1) - \ell_1 \end{cases} \quad t > T_1. \quad (24)$$

Since  $\dot{e}_1 = k_1 \text{sign}(\tilde{e}_1)$ , the system converges in fixed time. The value of  $\ell_1$  as the integral term of the sign function of the converged system is equal to zero. So we have  $\dot{e}_1 = \dot{e}_2 = \dot{e}_3 = \mathbf{0}$  when  $t > T_1$ .

The new state equation is obtained by replacing the observed values with the actual values as

$$\begin{cases} \dot{\hat{X}}_1 = T \hat{X}_2 \\ \dot{\hat{X}}_2 = -\chi^{-1} \Upsilon X_2 + \chi^{-1} \bar{v} + \hat{\delta}^* \end{cases} \quad (25)$$

## 4 Backstepping Controller Design

### 4.1 Control Law Design

Define two sliding surfaces  $s_1$  and  $s_2$

$$\begin{cases} s_1 = e_1 + k_1 C_1 \\ \dot{C}_1 = \gamma_1 \text{sig}^\alpha(e_1) + \eta_1 \text{sig}^\beta(e_1), \end{cases} \quad (26)$$

$$\begin{cases} s_2 = e_2 + k_2 C_2 \\ \dot{C}_2 = \gamma_2 \text{sig}^\alpha(e_2) + \eta_2 \text{sig}^\beta(e_2), \end{cases} \quad (27)$$

where  $e_1 = \hat{X}_1 - X_{1d}$ ,  $e_2 = \hat{X}_2 - X_{2d}$ ;  $C_1, C_2$  are synovial variables;  $\alpha, \beta, \gamma_i, \beta_i, k_i, \eta_i$  are all positive constants and satisfy  $0 < \alpha < 1, \beta > 1$ .  $X_{2d}$  is the newly introduced state variable whose expression will be derived by backstepping.

If the sliding mode surfaces  $s_1$  and  $s_2$  satisfy  $\dot{s}_1 = \dot{s}_2 = \mathbf{0}$  then we have

$$\begin{cases} \dot{e}_1 = -k_1 \gamma_1 \text{sig}^\alpha(e_1) - k_1 \eta_1 \text{sig}^\beta(e_1) \\ \dot{e}_2 = -k_2 \gamma_2 \text{sig}^\alpha(e_2) - k_2 \eta_2 \text{sig}^\beta(e_2). \end{cases} \quad (28)$$

It follows from Lemma 1 that  $e_1, e_2$  all converge in fixed time. Therefore, the design goal of the controller is to make the first derivative of the sliding mode surface zero.

Combine (25) to differentiate the two sliding mode surfaces separately

$$\begin{cases} \dot{s}_1 = \dot{\hat{X}}_1 - \dot{X}_{1d} + k_1 \dot{C}_1 \\ \quad = T(s_2 - k_2 C_2 + X_{2d}) - \dot{X}_{1d} + k_1 \dot{C}_1 \\ \quad = T(s_2 + X_c - k_2 C_2 + X_{2d} - X_c) \\ \quad \quad - \dot{X}_{1d} + k_1 \dot{C}_1 \\ \dot{s}_2 = \dot{\hat{X}}_2 - \dot{X}_{2d} + k_2 \dot{C}_2 \\ \quad = -\chi^{-1} \Upsilon X_2 + \chi^{-1} \bar{\tau} + \hat{\delta}^* - \dot{X}_{2d} + k_2 \dot{C}_2 \end{cases}, \quad (29)$$

where  $X_c$  is the virtual control input with the following expression,  $\lambda_{11}, \lambda_{12}$  are positive constants

$$X_c = k_2 C_2 - T^{-1} k_1 \dot{C}_1 + T^{-1} \dot{X}_{1d} - \lambda_{11} \text{sig}^\alpha(s_1) - \lambda_{12} \text{sig}^\beta(s_1). \quad (30)$$

To reduce the computational burden caused by direct differentiation of dummy variables, the state variable  $X_{2d}$  is introduced [19],  $X_{2d}$  denotes the filtered value of  $X_c$  after passing a first-order low-pass filter at a time constant of  $\sigma$ , and the expression as

$$\sigma \dot{X}_{2d} = \text{sig}^\alpha(X_c - X_{2d}) + \text{sig}^\beta(X_c - X_{2d}). \quad (31)$$

Combined with the control objective, the control rate of the designed system is

$$\begin{aligned} \tau &= \text{sat}(\tau_0), \\ \tau_0 &= \chi[\chi^{-1} \Upsilon X_2 - \hat{\delta}^* + \dot{X}_{2d} - k_2 \dot{C}_2 \\ &\quad - \lambda_{21} \text{sig}^\alpha(s_2) - \lambda_{22} \text{sig}^\beta(s_2) - T s_1], \end{aligned} \quad (32)$$

where  $\lambda_{21}, \lambda_{22}$  are positive constants.

For Eq. (25), under the premise of satisfying Assumptions 1–4, the closed-loop system of SGFTUUB can be obtained by designing the above virtual control rate and backstepping controller, combined with the nonlinear first-order low-pass filter and observer.

### 4.2 Stability Analysis

The Lyapunov function  $V$  is chosen as

$$V = \frac{1}{2}(s_1^2 + s_2^2 + z^2), \quad (33)$$

where  $z = X_{2d} - X_c$  represents the filtering error. The first derivative is denoted as

$$\dot{z} = \dot{X}_{2d} - \dot{X}_c = -\frac{1}{\sigma} \text{sig}^\alpha(z) - \frac{1}{\sigma} \text{sig}^\beta(z) - \dot{X}_c. \quad (34)$$

**Remark 5** The stability of the observer has been proved in section III, so only the stability of the controller is discussed next.

Combining Eq. (30) and Assumption 2,3, we know that the first derivative of the virtual control rate  $X_c$  is bounded, that is,  $|\dot{X}_c| \leq |\delta_{X_c}|$ , where  $\delta_{X_c}$  is a positive constant vector.

Taking the derivative of Eq. (33) concerning time  $t$  and combining Eqs. (29), (32), (34) and  $\|T\| = \frac{1}{\cos \theta} \geq 1$  from (2), we have

$$\begin{aligned} \dot{V} &= s_1 \dot{s}_1 + s_2 \dot{s}_2 + z \dot{z} \\ &\leq s_1 T(s_2 - \lambda_{11} \text{sig}^\alpha(s_1) - \lambda_{12} \text{sig}^\beta(s_1) + z) \\ &\quad + s_2(-T s_1 - \lambda_{21} \text{sig}^\alpha(s_2) - \lambda_{22} \text{sig}^\beta(s_2)) \\ &\quad + z(-\frac{1}{\sigma} \text{sig}^\alpha(z) - \frac{1}{\sigma} \text{sig}^\beta(z) + \delta_{X_c}) \\ &\leq -\lambda_{11}(s_1^2)^{\frac{1+\alpha}{2}} - \lambda_{12}(s_1^2)^{\frac{1+\beta}{2}} + s_1 z - \lambda_{21}(s_2^2)^{\frac{1+\alpha}{2}} \\ &\quad - \lambda_{22}(s_2^2)^{\frac{1+\beta}{2}} - \frac{1}{\sigma}(z^2)^{\frac{1+\alpha}{2}} - \frac{1}{\sigma}(z^2)^{\frac{1+\beta}{2}} + z \delta_{X_c}, \end{aligned} \quad (35)$$

Young’s inequality  $2xy \leq x^2 + y^2$  can be further transformed into

$$\begin{aligned} \dot{V} &\leq -\lambda_{11}(s_1^2)^{\frac{1+\alpha}{2}} - \lambda_{12}(s_1^2)^{\frac{1+\beta}{2}} - \lambda_{21}(s_2^2)^{\frac{1+\alpha}{2}} \\ &\quad - \lambda_{22}(s_2^2)^{\frac{1+\beta}{2}} + \frac{1}{2}s_1^2 + z^2 - \frac{1}{\sigma}(z^2)^{\frac{1+\alpha}{2}} \\ &\quad - \frac{1}{\sigma}(z^2)^{\frac{1+\beta}{2}} + \frac{1}{2}\delta_{X_c}^2 \\ &\leq -\lambda_{11}(s_1^2)^{\frac{1+\alpha}{2}} - \lambda_{21}(s_2^2)^{\frac{1+\alpha}{2}} - (\lambda_{12} - \frac{1}{2})(s_1^2)^{\frac{1+\beta}{2}} \\ &\quad - (\lambda_{22} - \frac{1}{2})(s_2^2)^{\frac{1+\beta}{2}} - \frac{1}{\sigma}(z^2)^{\frac{1+\alpha}{2}} \\ &\quad - (\frac{1}{\sigma} - 1)(z^2)^{\frac{1+\beta}{2}} + \frac{1}{2}\delta_{X_c}^2, \end{aligned} \quad (36)$$

when the parameters of the designed controller satisfy  $\{\lambda_{11}, \lambda_{21} > 0; \lambda_{12}, \lambda_{22} > \frac{1}{2}; \frac{1}{\sigma} > 1\}$ , let

$$\begin{aligned} M &= \min(\lambda_{11}, \lambda_{21}), \\ N &= \min(\lambda_{12} - \frac{1}{2}, \lambda_{22} - \frac{1}{2}), \\ P &= \frac{1}{\sigma} - 1, \end{aligned} \quad (37)$$

substitute in the above equation as

$$\begin{aligned} \dot{V} &\leq -M \sum_{i=1}^2 (s_i^2)^{\frac{1+\alpha}{2}} - N \sum_{i=1}^2 (s_i^2)^{\frac{1+\beta}{2}} - P(z^2)^{\frac{1+\alpha}{2}} \\ &\quad - P(z^2)^{\frac{1+\beta}{2}} + \frac{1}{2}\delta_{X_c}^2. \end{aligned} \quad (38)$$

**Lemma 2** [10] *If there exists a positive real number  $x_1, x_2, \dots, x_n \geq 0$  with exponent  $k > 0$ , then there is*

$$\begin{aligned} & \max(n^{k-1}, 1)(x_1^k + x_2^k + \dots + x_n^k) \\ & \geq (x_1 + x_2 + \dots + x_n)^k. \end{aligned} \tag{39}$$

By Lemma 2 we have

$$\begin{aligned} \dot{V} & \leq -\min(M, P) \left( \sum_{i=1}^2 (s_i^2)^{\frac{1+\alpha}{2}} + (z^2)^{\frac{1+\alpha}{2}} \right) \\ & \quad - \min(N, P) \left( \sum_{i=1}^2 (s_i^2)^{\frac{1+\beta}{2}} + (z^2)^{\frac{1+\beta}{2}} \right) + \frac{1}{2} \delta_{X_c}^2 \\ & \leq -\min(M, P) \left( \sum_{i=1}^2 (s_i^2) + z^2 \right)^{\frac{1+\alpha}{2}} \\ & \quad - \min(N, P) 3^{\frac{1-\beta}{2}} \left( \sum_{i=1}^2 (s_i^2) + z^2 \right)^{\frac{1+\beta}{2}} + \frac{1}{2} \delta_{X_c}^2 \\ & \leq -H_1 V^{\frac{1+\alpha}{2}} - H_2 V^{\frac{1+\beta}{2}} + \Delta, \end{aligned} \tag{40}$$

where  $H_1 = \min(M, P)$ ;  $H_2 = 3^{\frac{1-\beta}{2}} \min(N, P)$ ;  $\Delta = \frac{1}{2} \delta_{X_c}^2$ . When appropriate control parameters are chosen and  $M, N, P$  is positive, it follows from Lemma 1 that the Lyapunov function  $V$  is semi-global fixed-time uniform ultimate boundedness and has

$$T_V \leq \frac{2}{H_1(2^{(1+\alpha)/2} - 1)(1 - \alpha)} + \frac{2}{H_2(\beta - 1)}, \tag{41}$$

where  $T_V$  is the convergence time of  $V$ , The convergence time  $T_t$  of Eq. (29) is satisfied as

$$T_t \leq T_V + T_1. \tag{42}$$

**Theorem 2** *The controller in this paper does not appear Zeno phenomenon during the whole control process.*

**Proof** Based on the measuring error  $e(t) = \tau(t) - \bar{\tau}(t_k)$  defined in event-triggered mechanism,  $\bar{\tau}(t_k)$  is a constant for  $t \in [t_k, t_{k+1})$ , we have

$$\dot{e}(t) = \dot{\tau}(t) - \dot{\bar{\tau}}(t_k) = \dot{\tau}(t), \tag{43}$$

which implies  $\dot{e}_i(t) \leq |\dot{\tau}_i(t)|$ .

Taking the derivative of (32) we have

$$\begin{aligned} \dot{\tau} & = \chi[\chi^{-1} \Upsilon \dot{X}_2 - \dot{\delta}^* + \ddot{X}_{2d} - k_2 \ddot{C}_2 \\ & \quad - \lambda_{21} \alpha |s_2|^{\alpha-1} \text{sign}(s_2) \\ & \quad - \lambda_{22} \beta |s_2|^{\beta-1} \text{sign}(s_2) - \dot{T} s_1 - T \dot{s}_1]. \end{aligned} \tag{44}$$

Given the continuity of  $\dot{\tau}$  and based on the Assumptions 1–4, Eq. (43) satisfies as

$$\exists \bar{h} > 0, |\dot{\tau}| \leq \bar{h}. \tag{45}$$

Therefore, we obtain

$$\begin{aligned} \int_{t_k}^{t_{k+1}} \dot{\tau}(t) dt & = \tau(t_{k+1}) - \tau(t_k) \\ & \leq \zeta |\bar{\tau}(t_k)| + \varsigma - \mathbf{0} \\ & \leq \bar{h}(t_{k+1} - t_k). \end{aligned} \tag{46}$$

That means

$$t_{k+1} - t_k \geq \frac{\zeta |\bar{\tau}(t_k)| + \varsigma}{\bar{h}} \geq \frac{\varsigma}{\bar{h}}, \tag{47}$$

it is proved that there is no Zeno phenomenon in the control process of the controller.  $\square$

## 5 Simulation

In this section, the proposed algorithm is applied to the airship model proposed in Sect. 2 to verify the effectiveness of the control algorithm.

The airship modeling parameter values involved in the simulation in MATLAB are:  $m = 9.4 \times 10^3$  kg,  $\rho = 0.088$  kg/m<sup>3</sup>,  $l = 38$  m,  $C_d = 0.5$ ,  $L_{ref} = 38$  m,  $S_{ref} = 1134$  m<sup>2</sup>,  $[I_x, I_y, I_z] = 10^6 \times [2, 5.5, 5.5]$ ,  $x_c = y_c = 0$ ,  $z_c = 0.5$  m,  $G = 91556$  N,  $B = 91556$  N,  $a_1 = 73.5$ ,  $a_2 = 62.5$ ,  $b = 19$ .

The controller parameters are set as follows:  $\zeta_1 = \zeta_2 = \zeta_3 = \zeta_4 = \zeta_5 = \zeta_6 = 0.01$ ,  $\varsigma_1 = \varsigma_2 = \varsigma_3 = \varsigma_4 = \varsigma_5 = \varsigma_6 = 5$ ,  $\alpha = 0.8$ ,  $\alpha_1 = \alpha_2 = \alpha_3 = \alpha_4 = 0.6$ ,  $\beta = 1.2$ ,  $\beta_1 = \beta_2 = \beta_3 = \beta_4 = 1.5$ ,  $\mu_1 = \varepsilon_1 = 1$ ,  $\mu_2 = \varepsilon_2 = 0.01$ ,  $\mu_3 = \mu_4 = \varepsilon_3 = \varepsilon_4 = 0.001$ ,  $\gamma_1 = \gamma_2 = k_1 = k_2 = 0.01$ ,  $\eta_1 = \eta_2 = 0.01$ ,  $\sigma = 0.6$ ,  $\lambda_{11} = \lambda_{21} = 0.4$ ,  $\lambda_{12} = \lambda_{22} = 0.6$ .

The desired trajectory and the desired attitude are:

$$\begin{bmatrix} x_d \\ y_d \\ z_d \\ \phi_d \\ \theta_d \\ \psi_d \end{bmatrix} = \begin{bmatrix} 2000 \sin(0.005t) + 2000 \cos(0.0025t) \\ 2000 \sin(0.0025t) + 2000 \cos(0.005t) \\ -0.1t - 18930 \\ 0 \\ \arctan 2(0.1, \sqrt{\dot{x}_d^2 + \dot{y}_d^2}) \\ \arctan 2(\dot{y}_d, \dot{x}_d) \end{bmatrix},$$



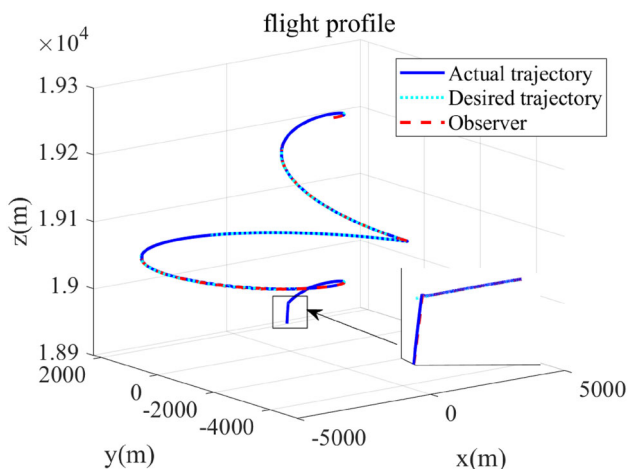


Fig. 2 Three-dimensional trajectory of the stratospheric airship

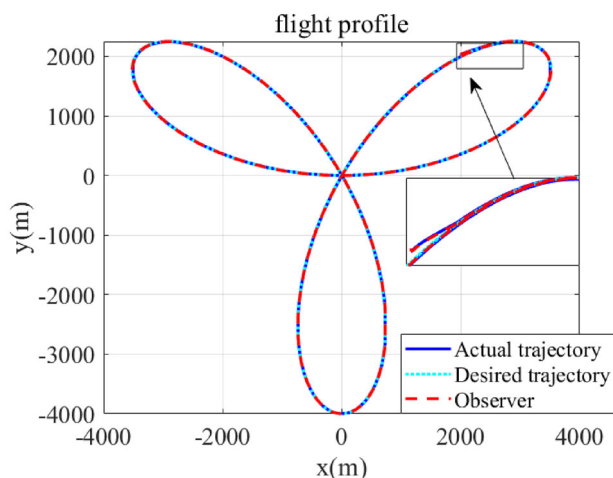


Fig. 3 The trajectory of the stratospheric airship in x-y plane

the initial state is:

$$\begin{bmatrix} x_0 \\ y_0 \\ z_0 \\ \phi_0 \\ \theta_0 \\ \psi_0 \end{bmatrix} = \begin{bmatrix} 2000 \text{ m} \\ 2040 \text{ m} \\ -18,900 \text{ m} \\ 0^\circ \\ 0^\circ \\ 30^\circ \end{bmatrix},$$

the unknown disturbance  $\chi^{-1}\Gamma(v_a) + f$  from the environment where  $f$  is set to:

$$f = -10^{-4} \times \begin{bmatrix} 2(1 + 0.1 \sin(t/60) + 0.2 \cos(t/60)) \\ 0.1(0.5 \sin(t/60) + \cos(t/60)) \\ 0.04(0.5 \sin(t/60) + 0.1 \cos(t/60)) \\ 0.5(1 + 0.1 \sin(t/60) + 0.2 \cos(t/60)) \\ 0.5(1 + 0.1 \sin(t/60) + 0.2 \cos(t/60)) \\ 2(1 + 0.1 \sin(t/60) + 0.2 \cos(t/60)) \end{bmatrix}.$$

In this subsection, the simulation results of the control algorithm are mainly as follows.

Figures 2 and 3 show the trajectory tracking of the stratospheric airship in three-dimensional space and an x-y plane. It can be seen that the proposed controller can make the stratospheric airship travel along the desired trajectory. Figures 4 and 5 illustrate the trajectory tracking performance of the proposed controller, while Figs. 6, 7 and 8 demonstrate the stability of the closed-loop system under the proposed control algorithm. Specifically, Fig. 4 shows the tracking error between the actual trajectory and the desired trajectory, and Fig. 5 shows the state response of the sliding surface.

Combined with Figs. 2, 9 and 10, it can be seen that there is a large trajectory error at the initial time, which leads to a significant control input in a short time. The controller reaches a saturated state to maximize the use of thrusters to make the airship get the desired trajectory. However, they

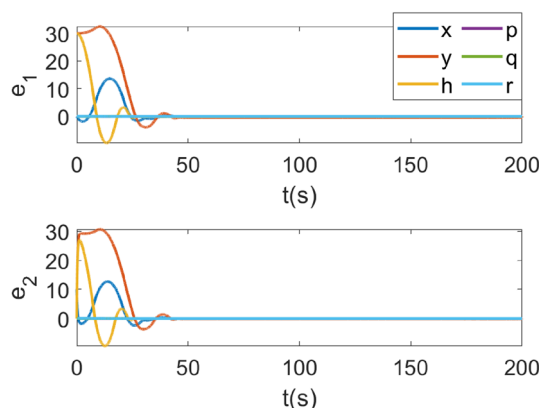


Fig. 4 Observation error curves for the six state variables

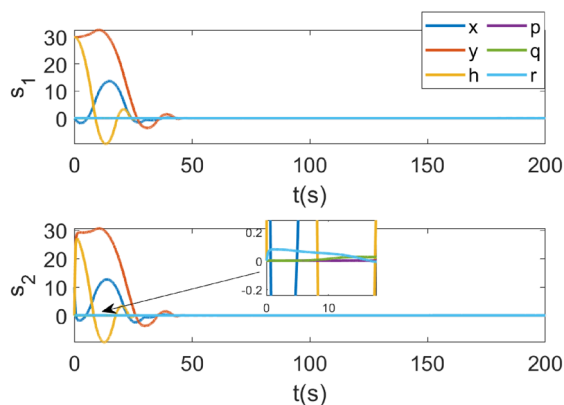


Fig. 5 Sliding surface state response curve

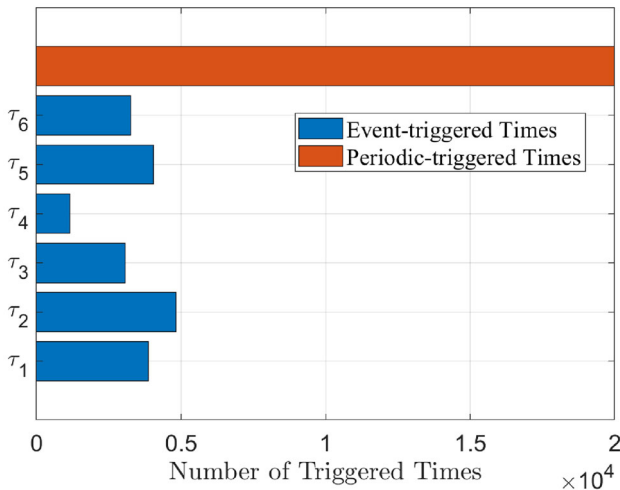


Fig. 6 Angular velocity curves during trajectory tracking of stratospheric airships

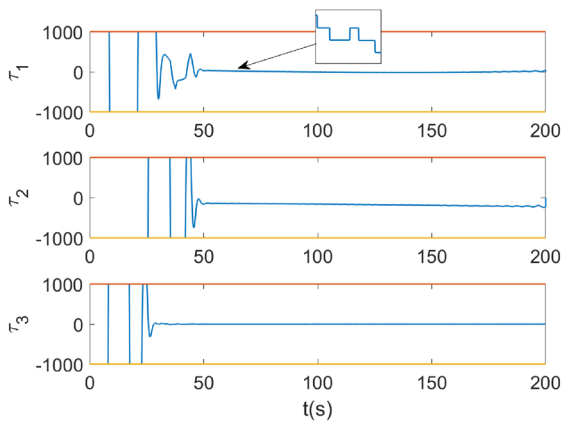


Fig. 7 Velocity curves during trajectory tracking of stratospheric airships

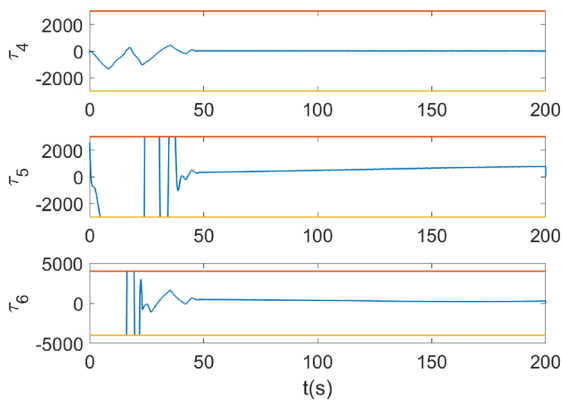


Fig. 8 Attitude angle curves during trajectory tracking of stratospheric airships

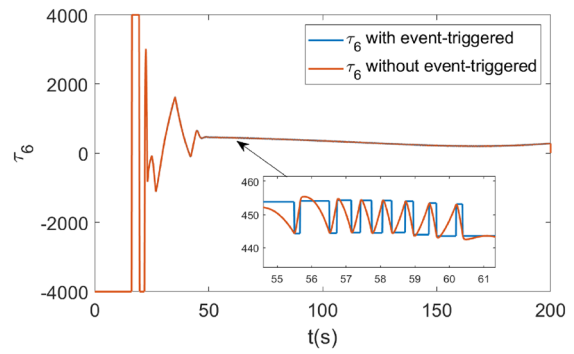


Fig. 9 Control force curves during trajectory tracking of stratospheric airships

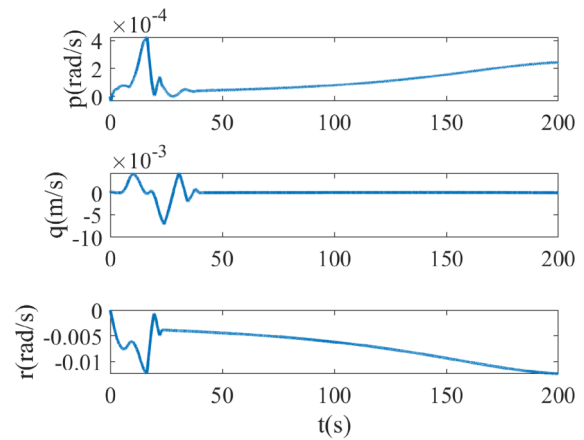


Fig. 10 Control moment curves during trajectory tracking of stratospheric airships

decrease rapidly after reaching the desired goal, which successfully indicates the effectiveness of the control algorithm in achieving the desired trajectory.

To verify the effectiveness of the event-triggered mechanism used in this paper, the controller model proposed is compared with the periodic control model after eliminating the event-triggered mechanism. By changing the control mode of time continuity into highly discretization control of condition trigger, the actuation frequency is successfully reduced, it can be seen from Fig. 11 that the operating frequency of the actuator under the action of the event-triggered mechanism controller is about 1/5 of that under periodic control. Figure 12 compares the periodic controller with the event-triggered controller by  $\tau_6$ . It is evident from the results that the event-triggered mechanism effectively reduces the operating frequency of the closed-loop system, thereby reducing the actuator damage of the stratospheric airship and increasing its air operation time.

To study the advantages of the controller in this paper, a comparative simulation is performed between different methods. The fixed-time trajectory tracking controller for multi-stratospheric airship formation in [26] is chosen as the com-

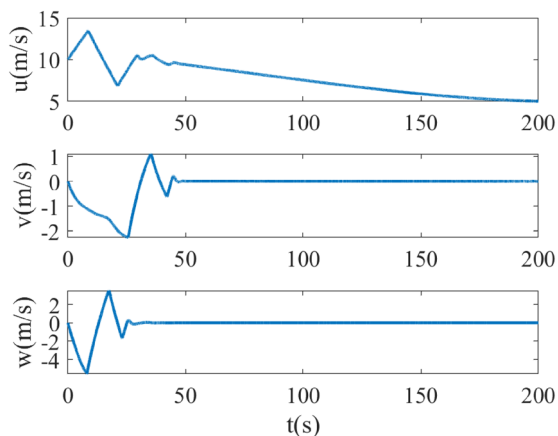


Fig. 11 Comparison of sensor working times based on event triggered and cycle triggered

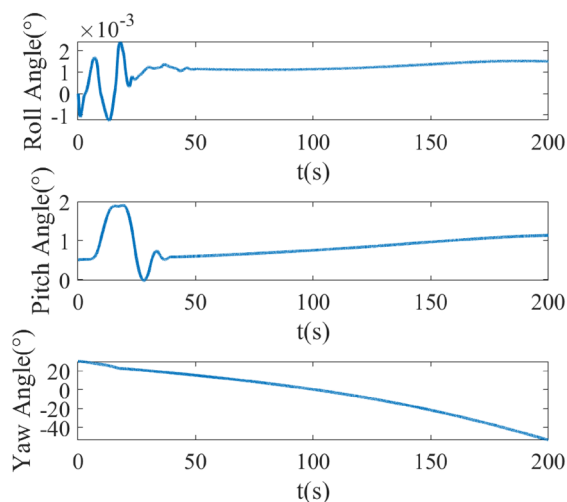


Fig. 12 Comparison of the influence of event triggering and no event triggering on control frequency

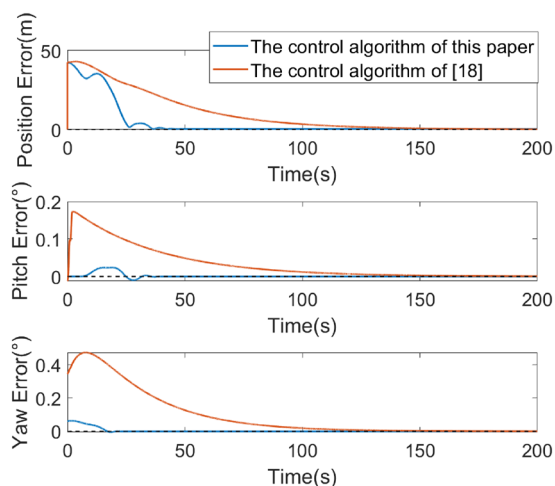


Fig. 13 Comparison of control errors for trajectory tracking of stratospheric airships with [26]

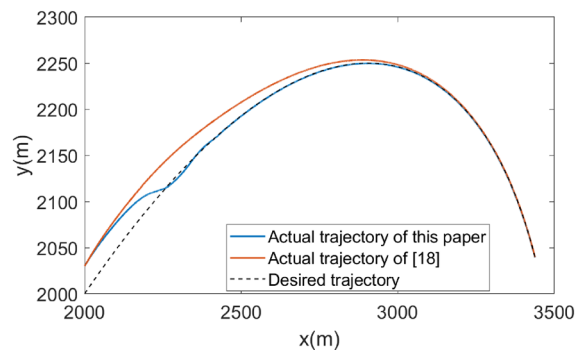


Fig. 14 Comparison of  $x$ - $y$  plane control trajectories for trajectory tracking of stratospheric airships with [26]

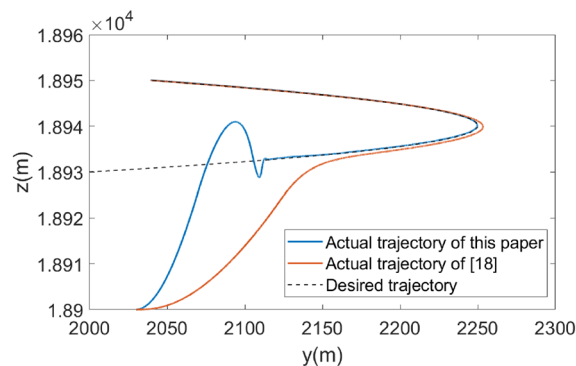


Fig. 15 Comparison of  $y$ - $z$  plane control trajectories for trajectory tracking of stratospheric airships with [26]

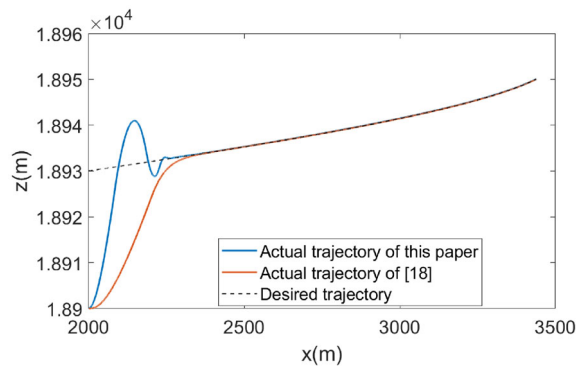


Fig. 16 Comparison of  $x$ - $z$  plane control trajectories for trajectory tracking of stratospheric airships with [26]

parison object. The controller parameters are  $k_{10} = k_{20} = k_{30} = \text{diag}[0.0140, 0.0100, 0.1000, 0, 0.4000, 0.0120]^T$ ,  $k_{40} = k_{50} = k_{60} = \text{diag}[0.0080, 0.0500, 0.1500, 0, 0.0080, 0.0500]^T$ ,  $k_{p0} = 21$ ,  $k_{q0} = 23$ , which is consistent with the control parameters of our method.

The results of the comparative simulation are shown in Figs. 13, 14, 15 and 16, where the comparison results of position variance error, pitch error, and yaw error are given in Fig. 13, and the trajectory in different directions is shown in Figs. 14, 15, and 16. It can be seen from Fig. 13 that

the transient response time of the control algorithm in this paper is smaller. Still, the trajectory overshoot of the control algorithm in this paper is relatively significant in Figs. 14, 15 and 16. This is because the computational input of the fixed-time controller exceeds the constraints of the actuator, resulting in saturation, which in turn deteriorates the control performance. To alleviate the impact of input saturation, some compensation methods can be introduced in future work.

## 6 Conclusion

In this paper, we propose an event-triggered trajectory tracking controller to address the issue of the unmeasurable airspeed of a stratospheric airship under unknown disturbances. A fixed-time observer is employed to estimate unmeasurable wind speed and unknown disturbances. A fixed-time controller is devised to ensure rapid convergence of the algorithm, and an event-triggered mechanism is implemented to reduce the working frequency of the actuator. The simulation results illustrate the successful and rapid trajectory tracking achieved by the proposed control algorithm and the closed-loop system remains bounded without any occurrence of Zeno phenomenon. The paper does not address the actuator saturation problem and constrained control issues. In future studies, additional constrained issues, such as the actuator saturation problem, will be considered.

**Author Contributions** Conceptualization, P.S. and Y.Z.; methodology, P.S.; software, P.S.; validation, P.S. and Y.Z.; formal analysis, P.S.; investigation, P.S.; resources, P.S.; data curation, P.S.; writing—original draft preparation, P.S.; writing?review and editing, Y.Z. and T.C.; visualization, P.S.; supervision, M.Z., T.C. and Z.Z.; project administration, M.Z. and Z.Z. All authors have read and agreed to the published version of the manuscript.

**Funding** This work was supported by the National Natural Science Foundation of China (Grant No. 52402509, Grant No. 62173016), and the the Fundamental Research Funds for the Central Universities (Grant No. 501JCGG2024129007, Grant No. 501JCGG2024103002).

## Declarations

**Conflict of interest** The authors declare no conflict of interest.

## References

- Basin M, Yu P, Shtessel Y (2017) Finite-and fixed-time differentiators utilising HOSM techniques. *IET Control Theory Appl* 11(8):1144–1152
- Bhat SP, Bernstein DS (2005) Geometric homogeneity with applications to finite-time stability. *Math Control Signals Syst* 17:101–127
- Chen L, Duan D, Sun D (2016) Design of a multi-vectored thrust aerostat with a reconfigurable control system. *Aerosp Sci Technol* 53:95–102. <https://doi.org/10.1016/j.ast.2016.03.011>
- Chen T, Zhu M, Zheng Z (2019) Asymmetric error-constrained path-following control of a stratospheric airship with disturbances and actuator saturation. *Mech Syst Signal Process* 119:501–522
- Cheng L, Zuo Z, Song J et al (2019) Robust three-dimensional path-following control for an under-actuated stratospheric airship. *Adv Space Res* 63(1):526–538
- Deng Y, Zhang X, Im N et al (2019) Event-triggered robust fuzzy path following control for underactuated ships with input saturation. *Ocean Eng* 186:106122
- Folsom RG (1956) Review of the pitot tube. *Trans Am Soc Mech Eng* 78(7):1447–1460
- Jiao J, Wang G (2016) Event triggered trajectory tracking control approach for fully actuated surface vessel. *Neurocomputing* 182:267–273
- Km Kang, Dj Kim (2019) Ship velocity estimation from ship wakes detected using convolutional neural networks. *IEEE J Select Top Appl Earth Observ Remote Sens* 12(11):4379–4388
- Li J, Yang Y, Hua C et al (2017) Fixed-time backstepping control design for high-order strict-feedback non-linear systems via terminal sliding mode. *IET Control Theory Appl* 11(8):1184–1193
- Liesk T, Nahon M, Boulet B (2013) Design and experimental validation of a nonlinear low-level controller for an unmanned fin-less airship. *IEEE Trans Control Syst Technol* 21(1):149–161. <https://doi.org/10.1109/TCST.2011.2178415>
- Liu L, Li X, Liu YJ et al (2021) Neural network based adaptive event trigger control for a class of electromagnetic suspension systems. *Control Eng Pract* 106:104675
- Nayler A (2003) Airship activity and development world-wide-2003. In: AIAA's 3rd annual aviation technology, integration, and operations (ATIO) Forum. p 6727
- Ni J, Liu L, Liu C et al (2017) Fixed-time leader-following consensus for second-order multiagent systems with input delay. *IEEE Trans Ind Electron* 64(11):8635–8646
- Pandey A, Parhi DR (2017) Optimum path planning of mobile robot in unknown static and dynamic environments using fuzzy-wind driven optimization algorithm. *Defenc Technol* 13(1):47–58
- Polyakov A (2012) Nonlinear feedback design for fixed-time stabilization of linear control systems. *IEEE Trans Autom Control* 57(8):2106–2110. <https://doi.org/10.1109/TAC.2011.2179869>
- Roney JA (2007) Statistical wind analysis for near-space applications. *J Atmos Solar-Terr Phys* 69(13):1485–1501
- Tran VP, Santoso F, Garratt MA (2021) Adaptive trajectory tracking for quadrotor systems in unknown wind environments using particle swarm optimization-based strictly negative imaginary controllers. *IEEE Trans Aerosp Electron Syst* 57(3):1742–1752
- Van M, Ceglarek D (2021) Robust fault tolerant control of robot manipulators with global fixed-time convergence. *J Frankl Inst* 358(1):699–722
- Wang X, Guo J, Tang S et al (2019) Fixed-time disturbance observer based fixed-time back-stepping control for an air-breathing hypersonic vehicle. *ISA Trans* 88:233–245
- Yan Z, Weidong Q, Yugeng X et al (2008) Stabilization and trajectory tracking of autonomous airship's planar motion. *J Syst Eng Electron* 19(5):974–981
- Yang Y, Hua C, Li J et al (2017) Robust adaptive uniform exact tracking control for uncertain Euler–Lagrange system. *Int J Control* 90(12):2711–2720
- Yuan J, Zhu M, Chen L et al (2020) Spatial trajectory tracking of a stratospheric airship with constraints. In: 2020 Chinese control and decision conference (CCDC). IEEE, pp 3951–3956
- Zhang G, Yao M, Xu J et al (2020) Robust neural event-triggered control for dynamic positioning ships with actuator faults. *Ocean Eng* 207:107292

25. Zhang L, Wei C, Wu R et al (2018) Fixed-time extended state observer based non-singular fast terminal sliding mode control for a VTVL reusable launch vehicle. *Aerosp Sci Technol* 82:70–79
26. Zhang Y, Zhu M, Chen T et al (2022) Distributed event-triggered fixed-time formation and trajectory tracking control for multiple stratospheric airships. *ISA Trans* 130:63–78
27. Zhang Z, Wu Y (2017) Fixed-time regulation control of uncertain nonholonomic systems and its applications. *Int J Control* 90(7):1327–1344
28. Zheng Z, Huo W (2013) Planar path following control for stratospheric airship. *IET Control Theory Appl* 7(2):185–201
29. Zheng Z, Zou Y (2016) Adaptive integral LOS path following for an unmanned airship with uncertainties based on robust RBFNN backstepping. *ISA Trans* 65:210–219. <https://doi.org/10.1016/j.isatra.2016.09.008>
30. Zheng Z, Huo W, Wu Z (2013) Autonomous airship path following control: theory and experiments. *Control Eng Pract* 21(6):769–788. <https://doi.org/10.1016/j.conengprac.2013.02.002>
31. Zheng Z, Yan K, Yu S et al (2017) Path following control for a stratospheric airship with actuator saturation. *Trans Inst Meas Control* 39(7):987–999. <https://doi.org/10.1177/0142331215625770>
32. Zhou B, Satyavada H, Baldi S (2017) Adaptive path following for unmanned aerial vehicles in time-varying unknown wind environments. In: 2017 American control conference (ACC). IEEE, pp 1127–1132
33. Zhou W, Fu J, Yan H et al (2021) Event-triggered approximate optimal path-following control for unmanned surface vehicles with state constraints. *IEEE Trans Neural Netw Learn Syst* 34:104–118
34. Zuo Z, Tian B, Defoort M et al (2017) Fixed-time consensus tracking for multiagent systems with high-order integrator dynamics. *IEEE Trans Autom Control* 63(2):563–570

**Publisher's Note** Springer Nature remains neutral with regard to jurisdictional claims in published maps and institutional affiliations.

Springer Nature or its licensor (e.g. a society or other partner) holds exclusive rights to this article under a publishing agreement with the author(s) or other rightsholder(s); author self-archiving of the accepted manuscript version of this article is solely governed by the terms of such publishing agreement and applicable law.